



An Efficient and Sustainable Approach to Decarboxylative Cross-Coupling Using Silica Coated Magnetic Copper Nanocatalyst for the Synthesis of Internal Alkynes

Manavi Yadav^{1,2}, Anju Srivastava², Rashmi Gaur¹, Radhika Gupta¹, Gunjan Arora¹ and Rakesh Kumar Sharma^{1*}

¹Green Chemistry Network Centre, Department of Chemistry, University of Delhi, New Delhi, India, ²Department of Chemistry, Hindu College, University of Delhi, Delhi, India

OPEN ACCESS

Edited by:

Moisés Canle,
University of A Coruña, Spain

Reviewed by:

Marie-Christine Scherrmann,
Université Paris-Saclay, France

Zhuohua Sun,
Beijing Forestry University, China

Luis Sarandeses,
University of A Coruña, Spain

*Correspondence:

Rakesh Kumar Sharma
rksharmagreenchem@hotmail.com

Specialty section:

This article was submitted to
Green and Sustainable Chemistry,
a section of the journal
Frontiers in Chemistry

Received: 10 September 2021

Accepted: 13 December 2021

Published: 17 January 2022

Citation:

Yadav M, Srivastava A, Gaur R, Gupta R, Arora G and Sharma RK (2022) An Efficient and Sustainable Approach to Decarboxylative Cross-Coupling Using Silica Coated Magnetic Copper Nanocatalyst for the Synthesis of Internal Alkynes. *Front. Chem.* 9:773855. doi: 10.3389/fchem.2021.773855

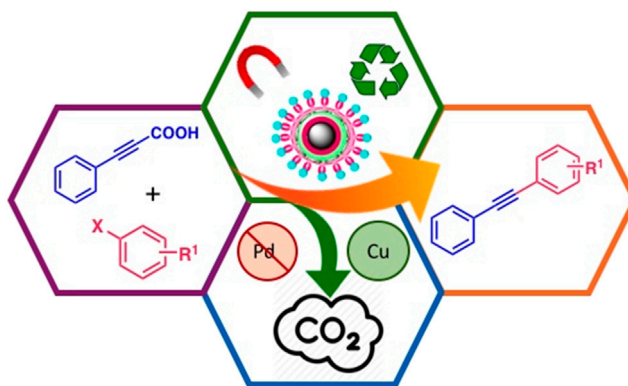
A highly efficient magnetically separable copper nanocatalyst has been developed for decarboxylative cross-coupling reaction for the alkylation of haloarenes using alkynoic acid as a reaction partner. The chemical nature, morphology, size, and magnetic properties of the prepared nanocatalyst were studied by SEM, TEM, EDS, FT-IR, VSM, and ICP techniques. Remarkably, this catalyst represents the first successful copper based heterogeneous system for this type of coupling that provides a low-cost, stable, and environmentally friendly magnetically recoverable entity that can be re-used for seven consecutive runs without appreciable loss in its catalytic performance.

Keywords: magnetic, copper, nanocatalyst, decarboxylative cross-coupling, heterogeneous catalyst

1 INTRODUCTION

Transition metal catalyzed cross-coupling reactions for the construction of carbon-carbon (C-C) bond are amongst the most powerful and efficient strategy for synthesizing essential organic compounds including bioactive compounds, natural products, and polymeric materials (Sonogashira, 2002; Tykwinski, 2003; Jutand, 2004). For this, various traditional cross-coupling reactions have been employed, however, these methods utilize organometallic compounds that bear Mg, Al, Zn, Sn, B, and Si, which create problem of metal contamination in the product. On comparison with the well-established cross-coupling reactions, decarboxylative cross-coupling reaction offers several benefits since it involves readily available carboxylic acid derivatives that do not encounter storage and handling difficulties and releases less-toxic carbon dioxide as the by-product that reduces the waste treatment costs. (Moon et al., 2008a; Moon et al., 2008b; Kim and Lee, 2009; Park et al., 2010; Zhang et al., 2010; Zhao et al., 2010; Li et al., 2011; Pan et al., 2011; Qu et al., 2011; Li et al., 2012; Tartaglia et al., 2012; Park and Lee, 2013; Reddy et al., 2013; Lee et al., 2016; Maaliki et al., 2016).

Due to the wide occurrence of alkyne moiety in natural products, pharmaceuticals, and molecular materials, enormous efforts have been devoted towards the synthesis of arylalkynes and conjugated enynes. (Brandsma, 2003; Negishi and Anastasia, 2003; Stang and Tykwinski, 2006; Chinchilla and Nájera, 2007). Of all, the Sonogashira coupling superseded all the traditional methods for synthesizing internal alkynes from nucleophilic terminal acetylenes. (Nicolaou et al., 2005;



GRAPHICAL ABSTRACT | Magnetic Silica core-shell copper nanocatalyst in the decarboxylative coupling for the synthesis of alkynes.

Stang, 2008). However, the formation of homo-coupled by-product and volatile liquid nature of terminal alkynes, are the major drawbacks which limit their utility in industrial applications. (Kolarovic et al., 2011). Therefore, the straightforward synthesis of arylalkynes with some other readily available substrates remained a practical challenge for many years. In recent times, decarboxylative cross-coupling of alkyne acids with haloarenes emerged as an attractive and practical solution. (Siemsen et al., 2000; Das et al., 2005; Feng and Loh, 2010; Jia and Jiao, 2010; Park et al., 2011).

To date, a number of homogeneous catalytic systems using palladium, copper and nickel catalysts have been developed for the decarboxylative coupling of alkyne acids with haloarenes. (Edwin Raja et al., 2016). However, most of them employ toxic phosphine ligands, and costly additives that are also air and moisture sensitive.

Despite tremendous success in the development of this methodology, till now, only few Pd-based heterogeneous catalysts have been reported for this reaction. (Pyo et al., 2013; Reddy et al., 2016). Moreover, these protocols have common problems associated with the palladium based catalysts, such as their high cost that limit their industrial applications. Nonetheless, exploring cost-effective methods to prepare highly stable, efficient, and recyclable heterogeneous catalysts still remain a challenging task in this field.

Therefore, employment of an economic and greener first row transition metal heterogenized catalyst is highly desirable. In this respect, copper-catalyzed systems have gained tremendous progress due to their economic attractiveness and good functional group tolerance (Ley and Thomas, 2003; Evano et al., 2008; Monnier and Taillefer, 2009). However, copper mediated synthesis of internal alkynes *via* decarboxylative coupling reaction is still less explored (Shang et al., 2009).

In line with current challenges arising from the demands of industrial and fine chemistry, an ideal catalyst should not only possess high activity and selectivity towards the targeted products but should be stable, environmental friendly, recyclable, and must be easy to recover from the reaction mixture. In view of these requirements, silica coated magnetic nanoparticles (SMNPs) appear to be an ideal solution as solid supports due to their

chemical inertness, robustness, easy magnetic recovery, recyclability, and environmentally benign nature (Rossi et al., 2014; Wang and Astruc, 2014; Sharma et al., 2016b).

Thus, in continuation of our ongoing research work on the development of nanocatalysts, and their applications in various organic transformations, (Sharma et al., 2015a; Sharma et al., 2015b; Sharma et al., 2016a; Sharma et al., 2016c; Arora et al., 2017; Gupta et al., 2017; Sharma et al., 2018), we herein describe the fabrication of a novel copper nanocatalyst with modified silica magnetic core-shell support for efficiently catalyzing decarboxylative coupling of alkyne acid with haloarenes.

2 MATERIALS AND METHODS

3-aminopropyltriethoxysilane (APTES), tetraethoxyorthosilicate (TEOS), and 4, 5-diazafluoren-9-one were procured from Sigma Aldrich. Ferric sulphate hydrate and ferrous sulphate heptahydrate were obtained from Sisco Research Laboratory (SRL). copper(I) iodide, Cs_2CO_3 , and toluene were purchased from Merck.

The prepared nanocatalyst was characterized using several techniques. X-ray diffraction (XRD) patterns were obtained from a D8 Discover Bruker AXS (Karlsruhe, Bundesland, Germany) diffractometer in the 2θ range of 10–80. For uniformity and morphology HR-TEM, FEI TECNAIF 30 transmission electron microscope with HAADF detector was used and operated at 300 kV. In order to study the chemical composition of the catalyst, X-ray energy dispersive spectroscopy (EDS) was carried out using Ametek EDAX system. Carl Zeiss India scanning electron microscope was used to investigate for analyzing the structural properties of prepared nanocomposites. EV-9, Microsense, ADE vibrating sample magnetometer was used to conduct magnetization measurements. The Fourier transform infrared spectra (FT-IR) of NPs were collected at every stage of synthesis using Perkin-Elmer Spectrum 2000. For the estimation of amount of copper in the catalyst and in the supernatant inductively coupled plasma (ICP) of PerkinElmer Optima 2100 DV was used. The products were confirmed by making use of Agilent gas chromatography-

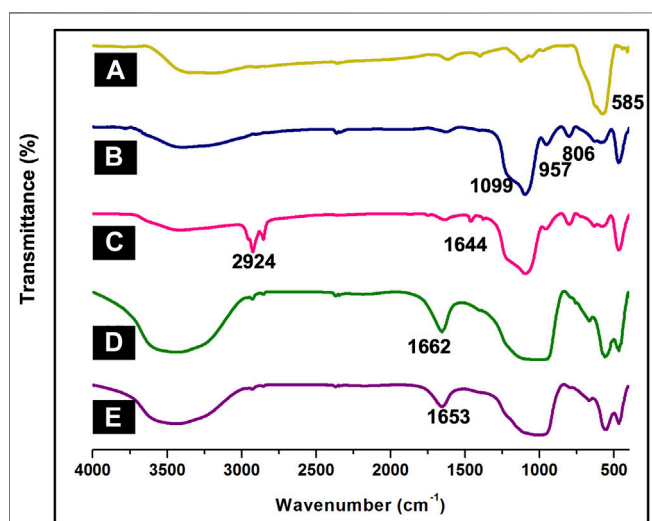
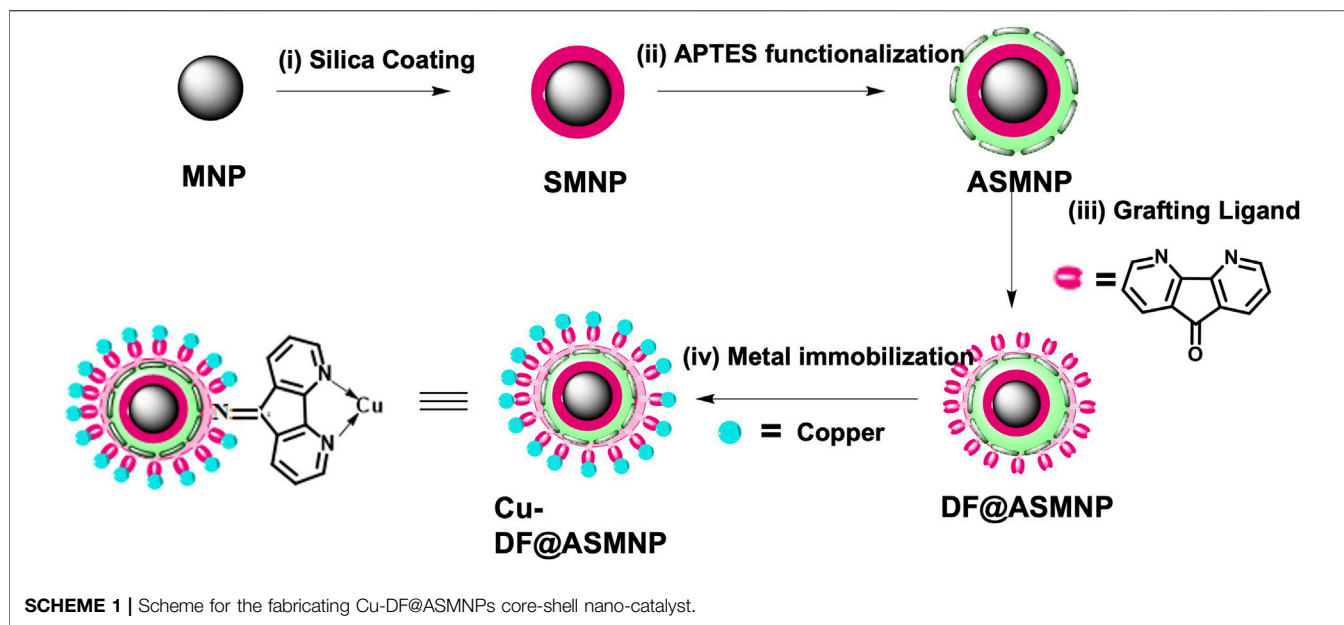


FIGURE 1 | FT-IR spectra of (A) MNPs, (B) SMNPs, (C) ASMNPs, (D) DF@ASMNPs, and (E) Cu-DF@ASMNPs.

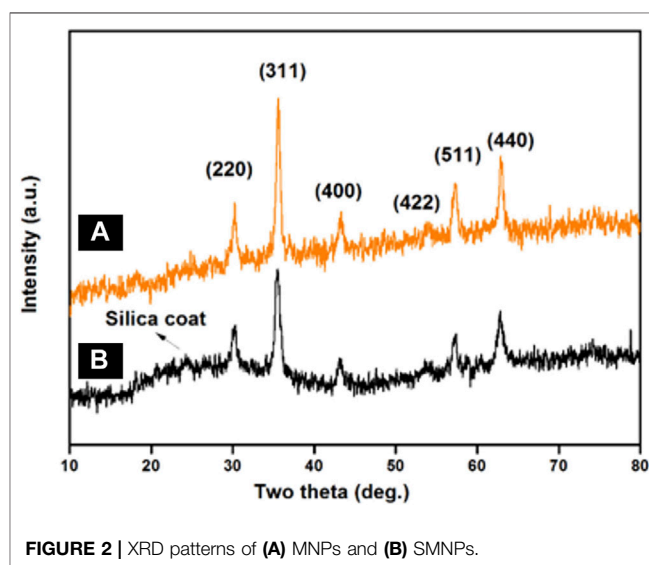


FIGURE 2 | XRD patterns of (A) MNPs and (B) SMNPs.

mass spectrometer with a HP-5MS 5% phenyl methyl siloxane capillary column (30.0 m × 0.25 mm × 0.25 μm) using helium as a carrier gas.

2.1 Synthesis of Cu-DF@ASMNPs

Firstly, MNPs were synthesized by co-precipitation technique. (Polshettiwar and Varma, 2009). For this, ferric sulphate (6.0 g) and ferrous sulphate (4.2 g) were dissolved in 250 ml distilled water and stirred at 60 C. To the obtained orange solution, 25% of NH₄OH (15 ml) was added dropwise and the solution was stirred vigorously for 30 min. The obtained black precipitates of MNPs were separated with external magnet and thoroughly washed with water and ethanol and finally dried under vacuum.

On to this, silica coating was performed *via* sol-gel approach to form SMNPs, (Zhang et al., 2011), which was further functionalized with the NH₂ linker, APTES. For silica coating, 0.5 g of MNPs were dissolved in 2.2 ml of 0.1 M HCl and dispersed in 200 ml ethanol and 50 ml water under sonication. Further, 5 ml NH₄OH was added followed by addition of 1 ml of TEOS under constant stirring at 60 C for 6 h to give SMNPs. These SMNPs were washed with ethanol and water. The functionalization with NH₂ linker was performed by adding 0.5 ml of APTES to the dispersed solution of 0.1 g of SMNPs in 100 ml of ethanol under constant stirring at 50 C for 6 h. 1 g of resulting APTES functionalized SMNPs (ASMNPs) were further reacted with a 0.75 mmol of bidentate ligand, 4, 5-diazafluoren-9-one (DF) in acetone at

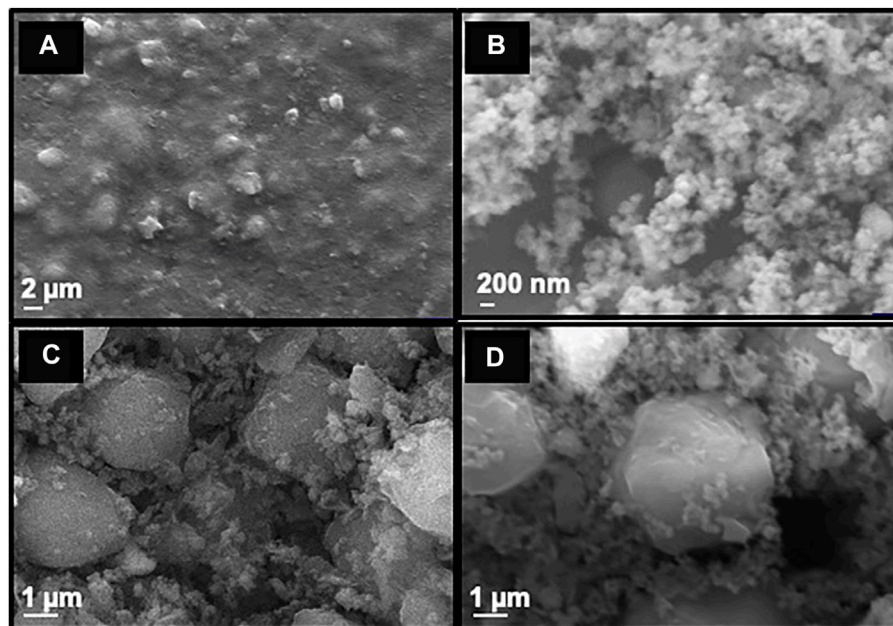


FIGURE 3 | SEM images of (A) MNPs, (B) SMNPs, (C) Fresh Cu-DF@ASMNPs and (D) Recovered Cu-DF@ASMNPs.

70°C for 3 h. The resulting DF@ASMNPs were washed with ethanol and dried under vacuum. To 1 g of DF@ASMNPs, 1.5 mmol of copper iodide was added and the solution was stirred for 3 h using acetone as solvent. The resulting nanocatalyst was magnetically recovered and thoroughly washed with deionized water and dried under vacuum to obtain the final catalyst Cu-DF@ASMNPs. (Scheme 1).

2.2 Cu-DF@ASMNPs Catalyzed Internal Alkynes Synthesis

For this, 10 ml of round bottom flask was flushed with nitrogen and to this, haloarene (0.5 mmol), alkyneic acid (0.6 mmol), Cu-DF@ASMNPs (25 mg), and Cs_2CO_3 (1.0 mmol) were added. Again, nitrogen was flushed, and toluene (2 ml) was added at room temperature. The temperature was raised to 100°C with continuous stirring for 12 h. On bringing to room temperature, the mixture was extracted with ethyl acetate. The reaction was monitored and analyzed by GC-MS.

3 RESULTS AND DISCUSSION

3.1 Characterization of Catalyst

3.1.1 FT-IR Spectroscopy

In order to analyze parent nanocomposite and its further functionalization, FT-IR spectroscopy was employed. A band was observed at 585 cm^{-1} in the IR-spectrum of MNPs depicting the Fe-O stretching absorption (Figure 1A). (Zhu et al., 2011) The intensity of this band reduced on silica-coating with the appearance of three new sharp bands in the region of 806 , 957 and $1,099\text{ cm}^{-1}$, corresponding to the symmetric Si-O-Si,

symmetric Si-O(H) and asymmetric Si-O-Si stretching vibrations respectively (Figure 1B) (Kooti and Afshari, 2012) Further functionalization of SMNPs with APTES resulted in absorption at $2,924\text{ cm}^{-1}$ and $1,644\text{ cm}^{-1}$, which corresponds to CH_2 and NH_2 from aminopropyl moiety of APTES (Figure 1C) (Yamaura et al., 2004) The immobilization of ligand DF onto ASMNPs was confirmed by the band at $1,662\text{ cm}^{-1}$ accredited to C=N stretching frequency (Figure 1D) and to this, metal was immobilized using CuI which shifted the prominent band at $1,662\text{ cm}^{-1}$ to a lower wavenumber indicating strong metal-ligand interaction (Figure 1E). (Masteri-Farahani and Tayyebi, 2011; Esmaeilpour et al., 2012).

3.1.2 XRD Studies

To assess the crystalline nature of synthesized MNPs and SMNPs, powder X-Ray diffraction measurements were carried out. For MNPs (Figure 2A), six characteristic peaks were observed at 2θ : 30.366° , 35.663° , 43.024° , 53.6° , 57.299° , and 62.865° corresponding to the (220), (311), (400), (422), (511) and (440) crystallographic faces of magnetite (Abu-Reziq and Alper, 2012). These peaks were in accordance with the standard XRD data provided by the Joint Committee on Powder Diffraction Standards (JCPDS) card number 19-0629 and is ascribed to inverse cubic spinel Fe_3O_4 crystal (Abu-Reziq et al., 2006). The average crystallite size of the MNPs was calculated by the Scherrer equation $\{D_{hkl} = K\lambda/(\beta_{hkl}\cos\theta)\}$, where D_{hkl} represents the size of the axis parallel to the (hkl) plane, k is a constant with a common value of 0.89 for spherical particles, λ is the wavelength of radiation, β_{hkl} is the full-width at half-maximum (FWHM) in radians, and θ is the diffraction angle. The mean crystallite size was found to be $\sim 10.6\text{ nm}$ for the (311) reflection. Besides these six diffraction peaks, a weak

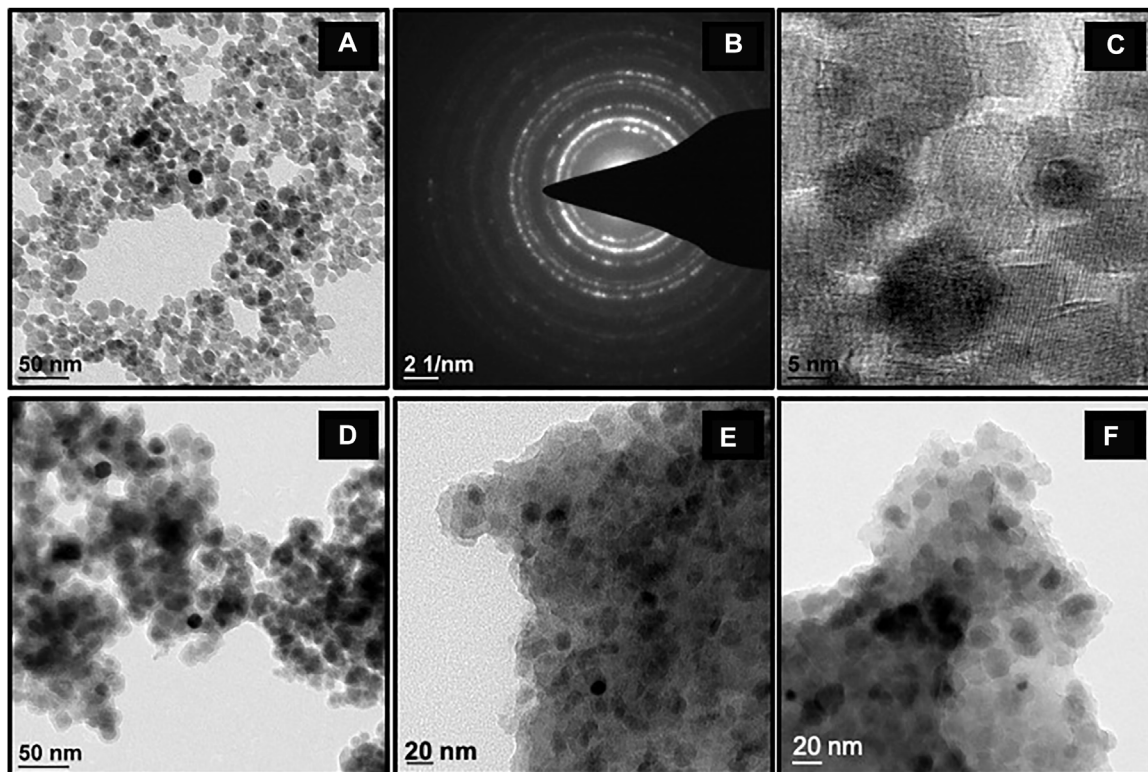


FIGURE 4 | TEM images of the nanoparticles obtained at different stages of synthesis: **(A)** MNPs, **(B)** SAED pattern of MNPs, **(C)** HR-TEM image of MNPs, **(D)** SMNPs, **(E)** Fresh Cu-DF@ASMNPs, and **(F)** Recovered Cu-DF@ASMNPs.

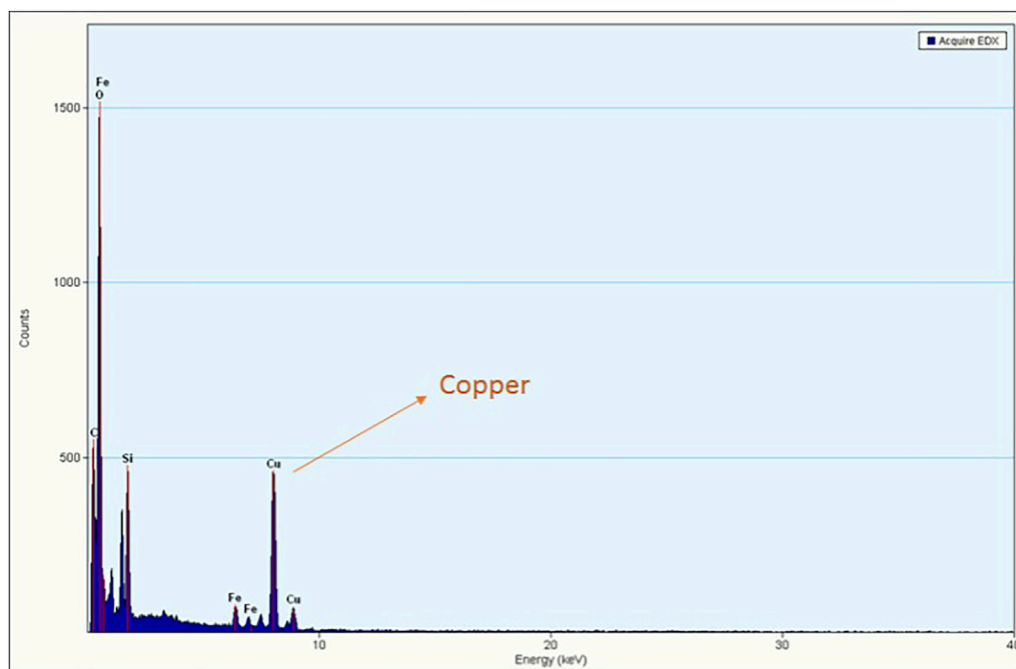
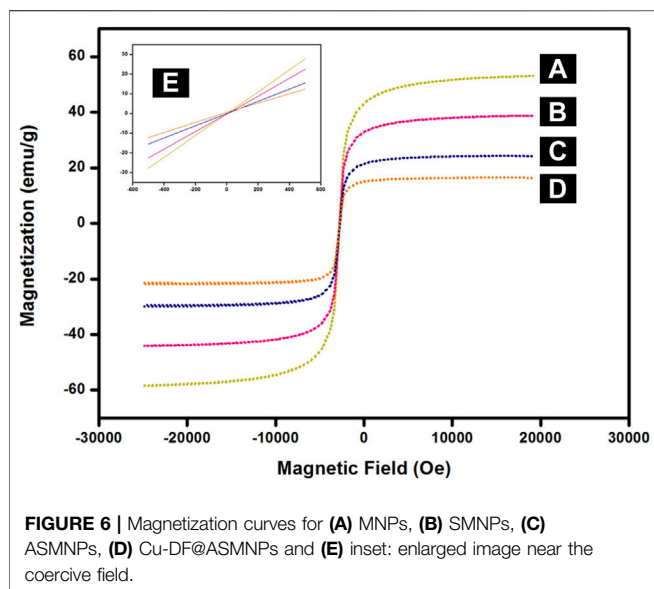


FIGURE 5 | EDS pattern of Cu-DF@ASMNPs.



broad hump at $2\theta = 20\text{--}24^\circ$ is observed in the XRD pattern of SMNPs showed in **Figure 2B**, which is attributed to amorphous silica (Zhang et al., 2012).

3.1.3 SEM Analysis

To investigate the topography of the synthesized nanoparticles, scanning electron microscopic (SEM) analysis was performed and it was found that the smooth surface of MNP (**Figure 3A**) turns spongy on silica coating (**Figure 3B**). The spherical morphology of the final Cu-DF@ASMNPs catalyst was seen with slight agglomeration and appears the same as that of

SMNP (**Figure 3C**). This suggested that the surface modification methods did not alter the morphology of the nanocatalyst. Besides this, the SEM image of the recovered catalyst (**Figure 3D**) also indicates that the reaction did not affect the morphology of the catalyst.

3.1.4 TEM Analysis

TEM studies were performed to study the morphological changes of the synthesized nanomaterials, **Figure 4A** depicts that MNPs are polydisperse in nature and display slight agglomeration (Wang et al., 2010; Wang et al., 2013). An array of bright diffraction rings was observed in the selected area electron diffraction pattern (SAED) (**Figure 4B**) which confirmed the crystalline nature of these nanocomposites and also in accordance with the resultant XRD pattern. The average interplanar distance of the MNPs was measured from a high-resolution transmission electron microscopy (HR-TEM) image and was found to be ~ 0.20 nm, which correlates with the (311) plane of inverse spinel Fe_3O_4 structure (**Figure 4C**). A dark core-shell of MNP, with an almost uniform silica coat of 4–5 nm thickness, was observed in the TEM image of SMNP (**Figure 4D**). TEM images of final catalyst and recovered catalyst are shown in **Figure 4E** and **Figure 4F** respectively, which further confirm that the structural morphology remain unchanged after the coupling reaction. In order to find the average particle size of MNPs, 52 colloidal aggregates were analyzed and it was found to be in the range of 10–11 nm (**Supplementary Figure S1**) which is in well accordance with the XRD results.

3.1.5 EDS Analysis and Metal Content Determination

Energy dispersive X-ray analysis was performed to detect the composition of the synthesized nanocomposites, and the EDS

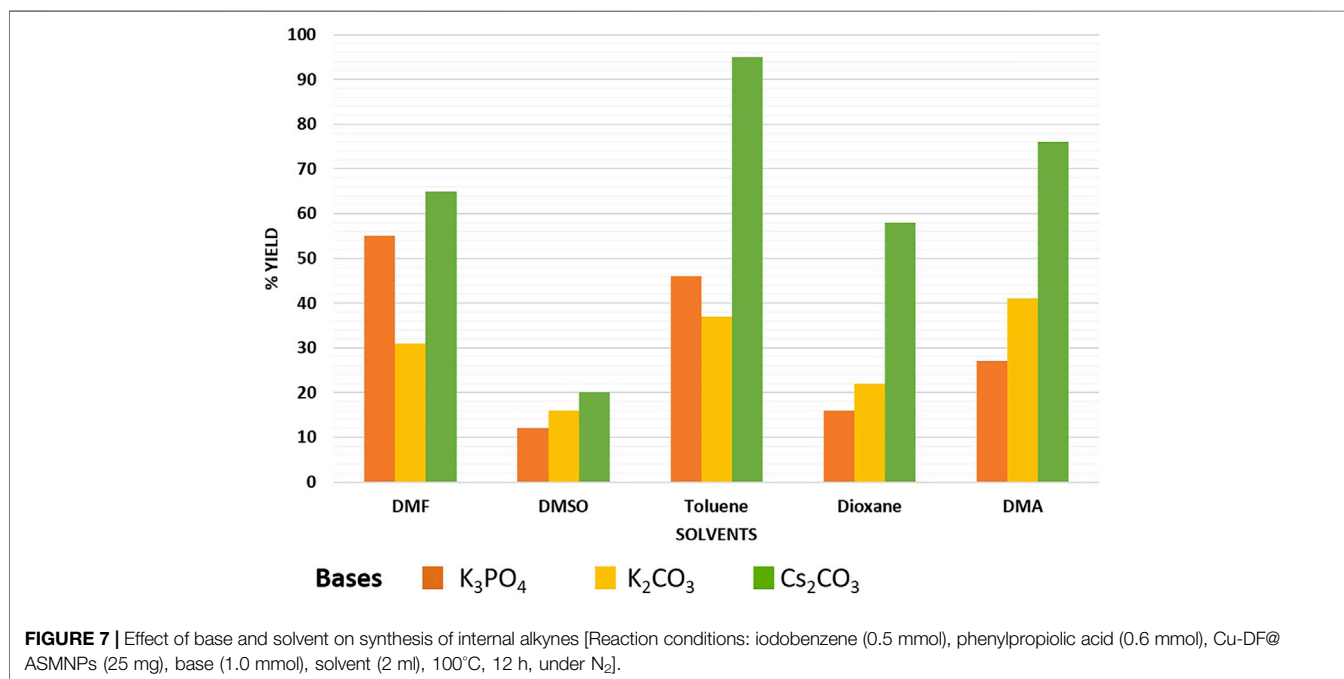
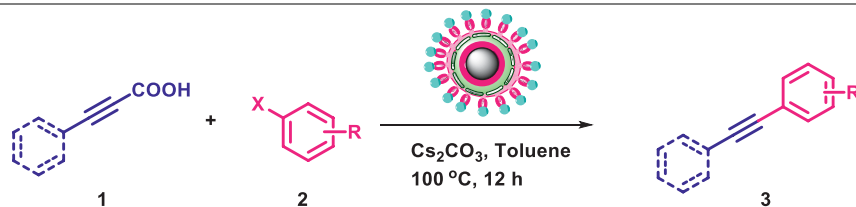
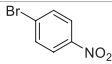
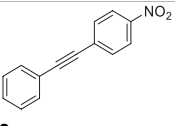
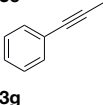


TABLE 1 | Scope of catalytic performance of the Cu-DF@ASMNP for synthesizing internal alkynes^a.

Entry	Haloarenes	Product	Yield ^b (%)	TON ^c
1		 3a	92	115
2		 3b	90	113
3 ^d		 3c	88/82 ^e	110
4		 3d	94/90 ^e	118
5		 3e	95	119
6		 3f	89/85 ^e	111
7		 3a	84	105
8		 3b	86	108
9		 3c	80	100

(Continued on following page)

TABLE 1 | (Continued) Scope of catalytic performance of the Cu-DF@ASMNP for synthesizing internal alkynes^a.

Entry	Haloarenes	Product	Yield ^b (%)	TON ^c
10		 3e	88/80 ^e	110
11		 3g	68	85

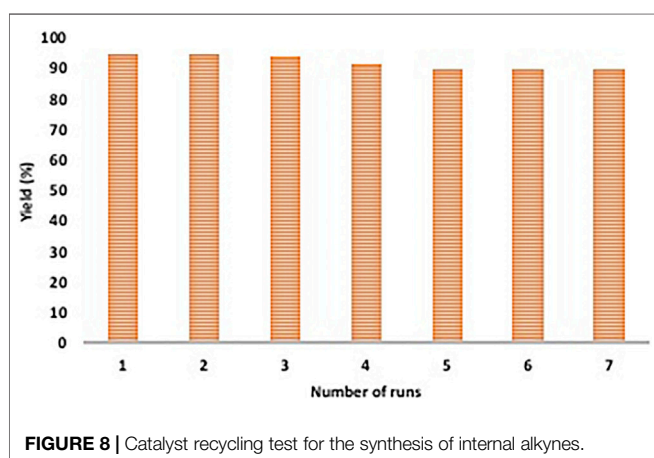
^aReaction conditions: Haloarene (0.5 mmol), alkynoic acid (0.6 mmol), Cu-DF@ASMNP (25 mg), Cs₂CO₃ (1.0 mmol), toluene (2 ml), 100°C, 12 h, under N₂.

^bGC-MS, yield.

^cTON, Calculated using the 0.3217 mmolg⁻¹ copper.

^eIsolated yield.

^dReaction was performed on large scale; Haloarene (5 mmol), alkynoic acid (6 mmol), Cu-DF@ASMNP (0.25 g), Cs₂CO₃ (10.0 mmol), toluene (10 ml), 100°C, 12 h, under N₂.



spectrum displayed well-defined peaks of copper, silicon and iron (Figure 5) that substantiate the effective grafting of copper on the Cu-DF@ASMNPs. Moreover, to determine the amount of copper present in the final catalyst, ICP analysis was conducted and the metal loading was found to be 0.3217 mmolg⁻¹.

3.1.6 VSM Analysis

The field-dependent magnetization measurement of synthesized nanocomposites is provided in Figure 6. The superparamagnetic behaviour of these nanoparticles was confirmed by their magnetization curves which display no hysteresis at room temperature. This was further corroborated by the inset in Figure 6 where both coercivity and remanence were negligible in the absence of an externally applied magnetic field. The saturation magnetization value of MNPs, SMNPs, ASMNPs, and Cu-DF@ASMNPs were found to be 59 emu g⁻¹, 40 emu g⁻¹, 29 emu g⁻¹, and 19 emu g⁻¹ respectively. This decrease in the M_s value is due to the non-magnetic nature of the functionalizing groups. (Hu et al., 2005; Digigow et al., 2014). Despite of lower value of magnetization, the net magnetism of Cu-DF@ASMNPs was high enough for its effortless removal *via* an external magnet.

3.2 Catalytic Studies

3.2.1 Optimization of the Reaction Conditions

In order to test the efficacy of the prepared nano-catalyst, Cu-DF@ASMNPs and to discover the optimal reaction conditions, phenylpropionic acid (0.6 mmol) and iodobenzene (0.5 mmol) were selected as the coupling partners. For the optimization of decarboxylative cross-coupling reaction, reaction parameters like solvent, base and catalytic amount were assessed. Figure 7 represent several combinations of base and solvent, and out of them highest yield was obtained when the base was Cs₂CO₃ (1 mmol), and toluene (2 ml) was the solvent. For the determination of the optimal catalytic amount, a blank test was carried out, where no significant yield was obtained. Although, the reaction gave product with 10 mg of catalyst and on increasing the amount of catalyst, significant increase in yield of the product was noticed. However, no noticeable increase in the product yield was found when 30 mg of catalyst was used and the best yield was achieved with 25 mg of catalyst (Supplementary Table S1). Also, the reaction was performed under diverse range of temperatures while keeping other parameters constant and 100 C was found to be the optimum temperature to carry out the coupling with 25 mg of synthesized catalyst (Supplementary Figure S2). Therefore, all the reactions were performed using toluene as the reaction solvent, Cs₂CO₃ as the base for 12 h at 100 C in the presence of 25 mg of Cu-DF@ASMNPs under N₂ atmosphere.

3.2.2 Catalytic Activity of Cu-DF@ASMNPs Catalyst for Decarboxylative Cross-Coupling of Alkynoic Acids With Haloarenes

To demonstrate the efficiency of this method, various haloarenes including iodo and bromo derivatives were coupled with phenylpropionic acid using the optimized reaction conditions (Table 1). To check the scope of this reaction, we initially examined a variety of iodoarenes possessing both activating and deactivating groups including methoxy, methyl, naphthyl, nitro, and chloro. It was observed that the reaction went smoothly for both electron donating and withdrawing groups on the

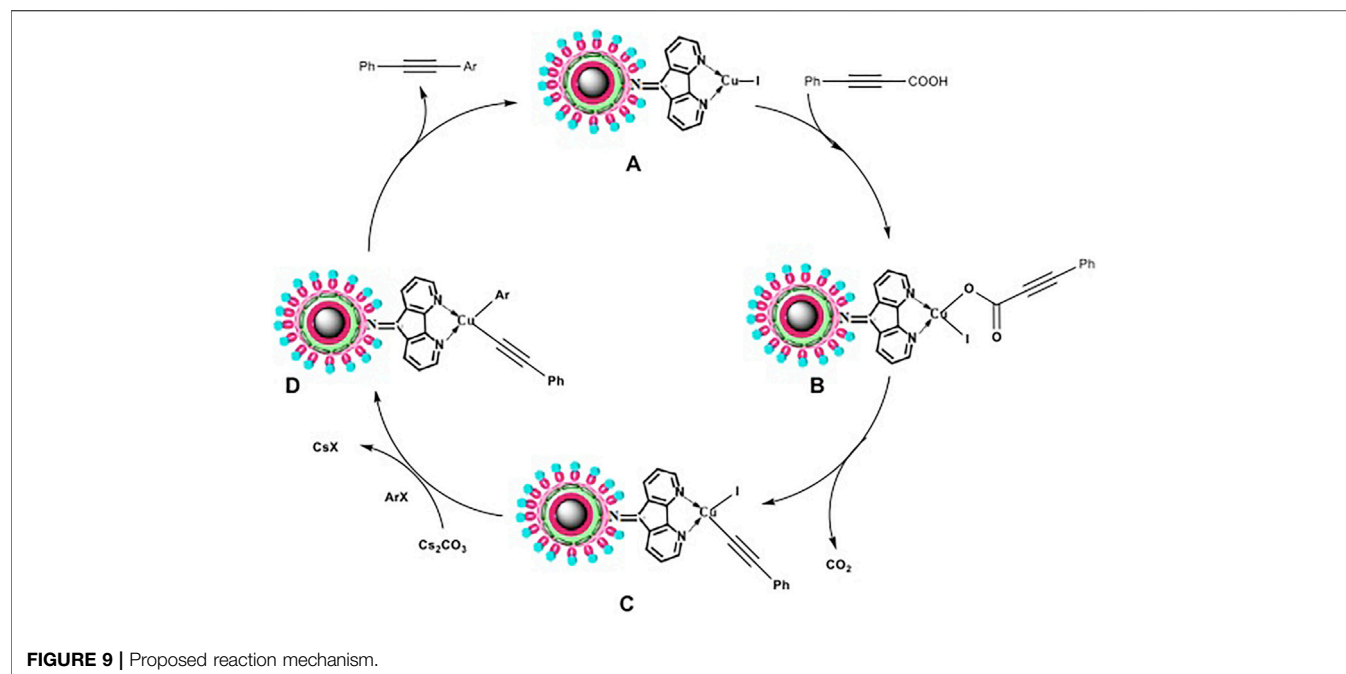
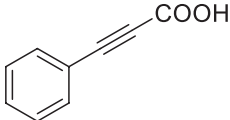
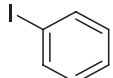
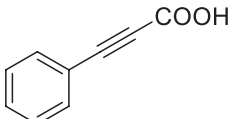
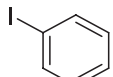
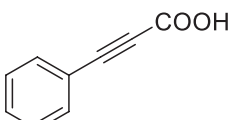
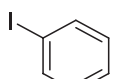
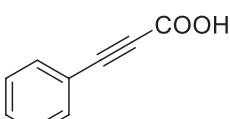
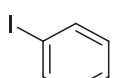
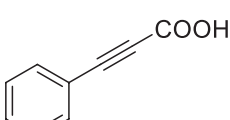
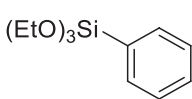
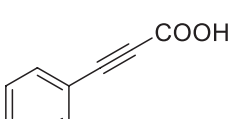
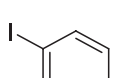
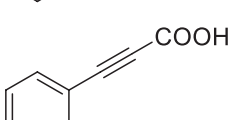
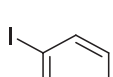
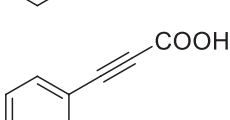
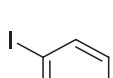


TABLE 2 | A comparison of the obtained results with previous published work for the synthesis of internal alkynes.

S.No	Acid	Coupling partner	Catalyst	Conditions	Yield (%)	Ref
1			Pd ₂ dba ₃ (5 mol%)	dppf (10 mol%), TBAF (6.0 equiv), NMP, 90°C, 1 h	88	Moon et al. (2008b)
2			Pd ₂ dba ₃ (2 mol%)	PPh ₃ (16 mol%), Ag ₂ O (1–3 equiv), LiI (3–6 equiv), DMF	64	Kim and Lee, (2009)
3			Pd (OAc) ₂	XPhos, Cs ₂ CO ₃ , THF, 80°C	70–95	Zhang et al. (2010)
4			Palladacycle (1 mol%)	Xphos (4 mol%), K ₂ CO ₃ (2 equiv), xylene/H ₂ O 120°C, 3 h	94	Li et al. (2013)
5			Pd (PPh ₃) ₂ Cl ₂ (1 mol%)	2 mol% of dppb, DMSO, 110°C, 2 h	96	Moon et al. (2008a)
6			[PdCl (allyl)] ₂ (2.5 mol%)	SPhos (7.5 mol%), TBAF (3.0 equiv), NMP/H ₂ O, 80°C, 14 h	84	Tartaggia et al. (2012)

(Continued on following page)

TABLE 2 | (Continued) A comparison of the obtained results with previous published work for the synthesis of internal alkynes.

S.No	Acid	Coupling partner	Catalyst	Conditions	Yield (%)	Ref
7			CuI (10 mol%)	1,10-Phen (10 mol%), Cs ₂ CO ₃ (1.5 equiv), DMF, 130°C, 24 h	99	Zhao et al. (2010)
8			CuI (2 mol%)	PPh ₃ (4 mol%), K ₂ CO ₃ (3 equiv), DMSO/H ₂ O 100°C, 24 h, under argon	97	Li et al. (2012)
9			CuI (0.5 mol%)/Fe(acac) ₃ (1 equiv)	K ₃ PO ₄ (2 equiv), DMSO (2 ml), 140°C, 24–48 h, under argon	98	Li et al. (2011)
10			CuSO ₄ ·5H ₂ O (10 mol%)	L (10 mol%), K ₂ CO ₃ (2 equiv), DMF, 130°C	90	Wang et al. (2016)
11			Ni(acac) ₂ (10 mol%)	1,10-Phen (10 mol%), CsF(1 equiv), CuF ₂ (1 Equiv)	90	Edwin Raja et al. (2016)
12 ^a			Pd-CNT (5 mol%)	DBU (2 equiv.), DMSO, 90°C, 12 h	95	Pyo et al. (2013)
13 ^a			Pd@PS (3 mol%)	DBU (3 equiv), DMF, 110°C, 12 h	66	Reddy et al. (2016)
14 ^a			Cu-DF@ ASMNP	Cs ₂ CO ₃ , toluene, 100°C, 12 h	92	This work

^aHeterogeneous catalyst.

iodoarene and excellent yields were obtained for various internal alkynes. For *p*-iodotoluene and *p*-iodoanisole the yield was similar, 90 and 88% respectively (entries 2 and 3). However, slight increase in yield was obtained when haloarene bearing electron withdrawing substituent was employed (entry 5).

To gauge the efficacy of reaction, more practical coupling partner aryl bromides were used. To our delight they also worked very well for this coupling reaction and both electron withdrawing as well as electron donating aryl bromides were efficiently converted into corresponding internal alkynes in excellent yields. To further assess the potential of the catalyst,

an aliphatic alkynoic acid, 2-butynoic acid (entry 11) was tested for this reaction but this afforded slightly lower yield. Isolated yields were obtained for few selected reactions consisting of haloarene bearing electron donating group (entry 3), neutral group (entry 4), a halogen substituent (entry 6) to check for any kind of interference, and electron withdrawing group (entry 10).

3.2.3 Catalytic Stability and Reusability

To test the reusability of catalyst, after each experiment (conducted under optimized conditions), the catalyst was magnetically separated, washed with ethyl acetate and ethanol

and dried under vacuum. This was then used to perform subsequent reactions. It was observed that the catalyst was active up to seven runs without any notable decrease in its performance (**Figure 8**). SEM and TEM images further confirmed the unaltered structure and morphology of the recovered catalyst (**Figure 3D** and **Figure 4F**).

3.2.4 Heterogeneity Test

In order to estimate the leaching rate and heterogeneous nature of the catalyst, two sets of corresponding experiments were conducted. A standard reaction was conducted for the first set where the catalyst was magnetically removed after completion of reaction, and filtrate was analyzed under ICP, which showed no leaching. A split test was performed with the second set, in which the standard reaction was conducted with catalyst for 2 hours, which roughly corresponds to 20% conversion by GC-MS. Afterwards, the nanocatalyst was magnetically separated from the reaction mixture and the reaction was further pursued. No coupling product in the reaction mixture was observed up to 10 hours under the same reaction conditions, which authenticate the truly heterogeneous nature of the nanocatalyst.

3.2.5 Plausible Mechanism

Figure 9 depicts the proposed mechanism that has been derived from earlier reports. (Okuro et al., 1993; Ray et al., 2008; Gonda et al., 2010; Lauterbach et al., 2010). The reaction between Cu-DF@ASMNPs A and alkynoic acid produces intermediate B, which undergoes decarboxylation to yield C, an alkynyl copper intermediate. Further addition of haloarene results in the formation of another intermediate D, which then undergoes reductive elimination, to give the product while regenerating the catalyst A.

Finally, in order to show the superiority of the synthesized catalyst, we compared our obtained results with the previously reported work (**Table 2**) and found that our catalyst was far more efficient in terms of reaction conditions, reaction time and catalytic recovery. Also, it is the first copper based heterogeneous system for synthesis of internal alkynes.

In summary, a highly effective palladium-free Cu-DF@ASMNPs nanocatalyst was fabricated successfully and applied

towards the synthesis of internal alkynes *via* decarboxylative cross-coupling reaction. These nanocomposites endowed low metal loading, high stability, and good functional group tolerance with excellent yields and high turn-over numbers. It is noteworthy that this catalytic system is the first report of copper based magnetic nanocatalyst that represents a practical and low-cost route to prepare internal alkynes. In addition, the effortless magnetic recovery and reusability of the catalyst for at least seven runs without any marked loss in its performance makes it an efficient protocol to produce a wide variety of unsymmetrical alkynes.

DATA AVAILABILITY STATEMENT

The original contributions presented in the study are included in the article/**Supplementary Material**, further inquiries can be directed to the corresponding author.

AUTHOR CONTRIBUTIONS

MY conceived the original idea. MY carried out the experiment and wrote the manuscript with support from AS, RG, GA, and RS supervised the work.

ACKNOWLEDGMENTS

One of the authors MY thanks USIC, University of Delhi, Delhi, India, for providing instrumentation facilities. MY is immensely grateful to ACS GCI for recognizing part of this work as best poster at the 21st Green Chemistry and Engineering Conference in Reston, VA.

SUPPLEMENTARY MATERIAL

The Supplementary Material for this article can be found online at: <https://www.frontiersin.org/articles/10.3389/fchem.2021.773855/full#supplementary-material>

REFERENCES

- Abu-Reziq, R., and Alper, H. (2012). Magnetically Separable Base Catalysts: Heterogeneous Catalysis vs. Quasi-Homogeneous Catalysis. *Appl. Sci.* 2 (2), 260–276. doi:10.3390/app2020260
- Abu-Reziq, R., Alper, H., Wang, D., and Post, M. L. (2006). Metal Supported on Dendronized Magnetic Nanoparticles: Highly Selective Hydroformylation Catalysts. *J. Am. Chem. Soc.* 128 (15), 5279–5282. doi:10.1021/ja060140u
- Arora, G., Yadav, M., Gaur, R., Gupta, R., and Sharma, R. K. (2017). A Novel and Template-free Synthesis of Multifunctional Double-Shelled Fe₃O₄-C Nanoreactor as an Ideal Support for Confined Catalytic Reactions. *ChemistrySelect* 2 (33), 10871–10879. doi:10.1002/slct.201701765
- Brandsma, L. (2003). *Best Synthetic Methods: Acetylenes, Allenes and Cumulenes*. Elsevier.
- Chinchilla, R., and Nájera, C. (2007). The Sonogashira Reaction: a Booming Methodology in Synthetic Organic Chemistry. *Chem. Rev.* 107 (3), 874–922. doi:10.1021/cr050992x
- Das, J. P., Roy, U. K., and Roy, S. (2005). Synthesis of Alkynyl and Vinyl Selenides via Selenodecarboxylation of Arylpropionic and Cinnamic Acids. *Organometallics* 24 (25), 6136–6140. doi:10.1021/om050504b
- Digigow, R. G., Dechézelles, J.-F., Dietsch, H., Geissbühler, I., Vanhecke, D., Geers, C., et al. (2014). Preparation and Characterization of Functional Silica Hybrid Magnetic Nanoparticles. *J. Magnetism Magn. Mater.* 362, 72–79. doi:10.1016/j.jmmm.2014.03.026
- Edwin Raja, G. C., Irudayanathan, F. M., Kim, H.-S., Kim, J., and Lee, S. (2016). Nickel-Catalyzed Hiyama-type Decarboxylative Coupling of Propiolic Acids and Organosilanes. *J. Org. Chem.* 81, 5244–5249. doi:10.1021/acs.joc.6b00883
- Esmailpour, M., Sardarian, A. R., and Javidi, J. (2012). Schiff Base Complex of Metal Ions Supported on Superparamagnetic Fe₃O₄@SiO₂ Nanoparticles: An Efficient, Selective and Recyclable Catalyst for Synthesis of 1,1-diacetates from

- Aldehydes under Solvent-free Conditions. *Appl. Catal. A: Gen.* 445–446, 359–367. doi:10.1016/j.apcata.2012.09.010
- Evano, G., Blanchard, N., and Toumi, M. (2008). Copper-mediated Coupling Reactions and Their Applications in Natural Products and Designed Biomolecules Synthesis. *Chem. Rev.* 108 (8), 3054–3131. doi:10.1021/cr8002505
- Feng, C., and Loh, T.-P. (2010). Palladium-catalyzed Decarboxylative Cross-Coupling of Alkynyl Carboxylic Acids with Arylboronic Acids. *Chem. Commun.* 46 (26), 4779–4781. doi:10.1039/c0cc00403k
- Gonda, Z., Tolnai, G. L., and Novák, Z. (2010). Dramatic Impact of Ppb Levels of Palladium on the "Copper-Catalyzed" Sonogashira Coupling. *Chem. - A Eur. J.* 16 (39), 11822–11826. doi:10.1002/chem.201001880
- Gupta, R., Yadav, M., Gaur, R., Arora, G., and Sharma, R. K. (2017). A Straightforward One-Pot Synthesis of Bioactive N-Aryl Oxazolidin-2-Ones via a Highly Efficient Fe₃O₄@SiO₂-Supported Acetate-Based Butylimidazolium Ionic Liquid Nanocatalyst under Metal- and Solvent-free Conditions. *Green. Chem.* 19 (16), 3801–3812. doi:10.1039/c7gc01414g
- Hu, A., Yee, G. T., and Lin, W. (2005). Magnetically Recoverable Chiral Catalysts Immobilized on Magnetite Nanoparticles for Asymmetric Hydrogenation of Aromatic Ketones. *J. Am. Chem. Soc.* 127 (36), 12486–12487. doi:10.1021/ja053881o
- Jia, W., and Jiao, N. (2010). Cu-catalyzed Oxidative Amidation of Propiolic Acids under Air via Decarboxylative Coupling. *Org. Lett.* 12 (9), 2000–2003. doi:10.1021/ol1004615
- Jutand, A. (2004). Dual Role of Nucleophiles in Palladium-Catalyzed Heck, Stille, and Sonogashira Reactions. *Pure Appl. Chem.* 76 (3), 565–576. doi:10.1351/pac200476030565
- Kim, H., and Lee, P. H. (2009). Palladium-Catalyzed Decarboxylative sp² Cross-Coupling Reactions of Aryl and Vinyl Halides and Triflates with $\text{I}^{\pm}, \text{I}^{\pm}$ -Ynoic Acids Using Silver Oxide. *Adv. Synth. Catal.* 351 (17), 2827–2832. doi:10.1002/adsc.200900502
- Kolarovic, A., Schmörch, M., and Mihovilovic, M. D. (2011). Tandem Catalysis: from Alkynoic Acids and Aryl Iodides to 1, 2, 3-triazoles in One Pot. *J. Org. Chem.* 76 (8), 2613–2618.
- Kooti, M., and Afshari, M. (2012). Phosphotungstic Acid Supported on Magnetic Nanoparticles as an Efficient Reusable Catalyst for Epoxidation of Alkenes. *Mater. Res. Bull.* 47 (11), 3473–3478. doi:10.1016/j.materresbull.2012.07.001
- Lauterbach, T., Livendahl, M., Rosellón, A., Espinet, P., and Echavarren, A. M. (2010). Unlikelihood of Pd-free Gold(I)-Catalyzed Sonogashira Coupling Reactions. *Org. Lett.* 12 (13), 3006–3009. doi:10.1021/ol101012n
- Lee, J.-H., Raja, G. C. E., Son, Y., Jang, J., Kim, J., and Lee, S. (2016). Nickel-catalyzed Oxidative Decarboxylative Coupling Reactions between Alkynyl Carboxylic Acids and Arylboronic Acids. *Tetrahedron Lett.* 57 (43), 4824–4828. doi:10.1016/j.tetlet.2016.09.054
- Ley, S. V., and Thomas, A. W. (2003). Modern Synthetic Methods for Copper-Mediated C(aryl)O, C(aryl)N, and C(aryl)S Bond Formation. *Angew. Chem. Int. Ed.* 42 (44), 5400–5449. doi:10.1002/anie.200300594
- Li, T., Qu, X., Zhu, Y., Sun, P., Yang, H., Shan, Y., et al. (2011). Synthesis of Diarylalkynes by Iron/Copper Co-Catalyzed Decarboxylative Sp² Sp² Coupling of Alkynyl Carboxylic Acids and Aryl Halides. *Adv. Synth. Catal.* 353 (14–15), 2731–2738. doi:10.1002/adsc.201100238
- Li, T., Sun, P., Yang, H., Zhu, Y., Yan, H., Lu, L., et al. (2012). Copper-catalyzed Decarboxylative Coupling of Aryl Halides with Alkynyl Carboxylic Acids Performed in Water. *Tetrahedron* 68 (32), 6413–6419. doi:10.1016/j.tet.2012.06.003
- Li, X., Yang, F., and Wu, Y. (2013). Palladacycle-Catalyzed Decarboxylative Coupling of Alkynyl Carboxylic Acids with Aryl Chlorides under Air. *J. Org. Chem.* 78 (9), 4543–4550. doi:10.1021/jo400574d
- Maaliki, C., Chevalier, Y., Thiery, E., and Thibonnet, J. (2016). Palladium and Copper Catalyzed Sonogashira Decarboxylative Coupling of Aryl Iodides and Alkynyl Carboxylic Acids. *Tetrahedron Lett.* 57 (30), 3358–3362. doi:10.1016/j.tetlet.2016.06.073
- Masteri-Farahani, M., and Tayyebi, N. (2011). A New Magnetically Recoverable Nanocatalyst for Epoxidation of Olefins. *J. Mol. Catal. A: Chem.* 348 (1), 83–87. doi:10.1016/j.molcata.2011.08.007
- Monnier, F., and Taillefer, M. (2009). Catalytic CC, CN, and CO Ullmann-type Coupling Reactions. *Angew. Chem. Int. Ed.* 48 (38), 6954–6971. doi:10.1002/anie.200804497
- Moon, J., Jang, M., and Lee, S. (2008a). Palladium-catalyzed Decarboxylative Coupling of Alkynyl Carboxylic Acids and Aryl Halides. *J. Org. Chem.* 74 (3), 1403–1406. doi:10.1021/jo802290r
- Moon, J., Jeong, M., Nam, H., Ju, J., Moon, J. H., Jung, H. M., et al. (2008b). One-Pot Synthesis of Diarylalkynes Using Palladium-Catalyzed Sonogashira Reaction and Decarboxylative Coupling of Sp Carbon and Sp² Carbon. *Org. Lett.* 10 (5), 945–948. doi:10.1021/ol703130y
- Negishi, E.-i., and Anastasia, L. (2003). Palladium-catalyzed Alkynylation. *Chem. Rev.* 103 (5), 1979–2018. doi:10.1021/cr020377i
- Nicolaou, K. C., Bulger, P. G., and Sarlah, D. (2005). Palladium-Catalyzed Cross-Coupling Reactions in Total Synthesis. *Angew. Chem. Int. Ed.* 44 (29), 4442–4489. doi:10.1002/anie.200500368
- Okuro, K., Furuune, M., Enna, M., Miura, M., and Nomura, M. (1993). Synthesis of Aryl- and Vinylacetylene Derivatives by Copper-Catalyzed Reaction of Aryl and Vinyl Iodides with Terminal Alkynes. *J. Org. Chem.* 58 (17), 4716–4721. doi:10.1021/jo00069a040
- Pan, D., Zhang, C., Ding, S., and Jiao, N. (2011). Phosphane-Free Copper-Catalyzed Decarboxylative Coupling of Alkynyl Carboxylic Acids with Aryl Halides under Aerobic Conditions. *Eur. J. Org. Chem.* 2011 (25), 4751–4755. doi:10.1002/ejoc.201101187
- Park, A., Park, K., Kim, Y., and Lee, S. (2011). Pd-catalyzed Carbonylative Reactions of Aryl Iodides and Alkynyl Carboxylic Acids via Decarboxylative Couplings. *Org. Lett.* 13 (5), 944–947. doi:10.1021/ol102993y
- Park, K., Bae, G., Moon, J., Choe, J., Song, K. H., and Lee, S. (2010). Synthesis of Symmetrical and Unsymmetrical Diarylalkynes from Propiolic Acid Using Palladium-Catalyzed Decarboxylative Coupling. *J. Org. Chem.* 75 (18), 6244–6251. doi:10.1021/jo101398a
- Park, K., and Lee, S. (2013). Transition Metal-Catalyzed Decarboxylative Coupling Reactions of Alkynyl Carboxylic Acids. *RSC Adv.* 3 (34), 14165–14182. doi:10.1039/c3ra41442f
- Polshettiwar, V., and Varma, R. S. (2009). Nanoparticle-supported and Magnetically Recoverable Palladium (Pd) Catalyst: a Selective and Sustainable Oxidation Protocol with High Turnover Number. *Org. Biomol. Chem.* 7 (1), 37–40. doi:10.1039/b817669h
- Pyo, A., Kim, J. D., Choi, H. C., and Lee, S. (2013). Ligand-free Palladium-Catalyzed Decarboxylative Coupling Reactions of Aryl Iodides and Alkynyl Carboxylic Acids. *J. Organomet. Chem.* 724, 271–274. doi:10.1016/j.jorganchem.2012.11.029
- Qu, X., Li, T., Sun, P., Zhu, Y., Yang, H., and Mao, J. (2011). Highly Effective Copper-Catalyzed Decarboxylative Coupling of Aryl Halides with Alkynyl Carboxylic Acids. *Org. Biomol. Chem.* 9 (20), 6938–6942. doi:10.1039/c1ob05969f
- Ray, L., Barman, S., Shaikh, M. M., and Ghosh, P. (2008). Highly Convenient Amine-free Sonogashira Coupling in Air in a Polar Mixed Aqueous Medium Bytrans- and cis-[(NHC)2PdX2] (X=Cl, Br) Complexes of N/O-Functionalized N-Heterocyclic Carbenes. *Chem. Eur. J.* 14 (22), 6646–6655. doi:10.1002/chem.200800301
- Reddy, C. B., Bharti, R., Kumar, S., and Das, P. (2016). Supported Palladium Nanoparticles-Catalyzed Decarboxylative Coupling Approaches to Aryl Alkynes, Indoles and Pyrrolines Synthesis. *RSC Adv.* 6 (75), 71117–71121. doi:10.1039/c6ra12046f
- Reddy, P. V., Srinivas, P., Annappurna, M., Bhargava, S., Wagler, J., Mirzadeh, N., et al. (2013). Phosphine-Free Palladium-Catalyzed Decarboxylative Coupling of Alkynylcarboxylic Acids with Aryl and Heteroaryl Halides. *Adv. Synth. Catal.* 355 (4), 705–710. doi:10.1002/adsc.201200876
- Rossi, L. M., Costa, N. J. S., Silva, F. P., and Wojcieszak, R. (2014). Magnetic Nanomaterials in Catalysis: Advanced Catalysts for Magnetic Separation and beyond. *Green. Chem.* 16 (6), 2906–2933. doi:10.1039/c4gc00164h
- Shang, R., Fu, Y., Wang, Y., Xu, Q., Yu, H.-Z., and Liu, L. (2009). Copper-Catalyzed Decarboxylative Cross-Coupling of Potassium Polyfluorobenzoates with Aryl Iodides and Bromides. *Angew. Chem.* 121 (49), 9514–9518. doi:10.1002/ange.200904916
- Sharma, R. K., Gaur, R., Yadav, M., Goswami, A., Zboril, R., and Gawande, M. B. (2018). An Efficient Copper-Based Magnetic Nanocatalyst for the Fixation of Carbon Dioxide at Atmospheric Pressure. *Sci. Rep.* 8 (1), 1901. doi:10.1038/s41598-018-19551-3

- Sharma, R. K., Gaur, R., Yadav, M., Rathi, A. K., Pechousek, J., Petr, M., et al. (2015a). Maghemite-Copper Nanocomposites: Applications for Ligand-free Cross-Coupling (C–O, C–S, and C–N) Reactions. *ChemCatChem*. 7 (21), 3495–3502. doi:10.1002/cctc.201500546
- Sharma, R. K., Yadav, M., Gaur, R., Gupta, R., Adholeya, A., and Gawande, M. B. (2016a). Synthesis of Iron Oxide Palladium Nanoparticles and Their Catalytic Applications for Direct Coupling of Acyl Chlorides with Alkynes. *ChemPlusChem*. 81 (12), 1312–1319. doi:10.1002/cplu.201600321
- Sharma, R. K., Yadav, M., Gaur, R., Monga, Y., and Adholeya, A. (2015b). Magnetically Retrievable Silica-Based Nickel Nanocatalyst for Suzuki-Miyaura Cross-Coupling Reaction. *Catal. Sci. Technol.* 5 (5), 2728–2740. doi:10.1039/c4cy01736f
- Sharma, R. K., Yadav, M., and Gawande, M. B. (2016b). “Silica-coated Magnetic Nano-Particles: Application in Catalysis,” in *Ferrites and Ferrates: Chemistry and Applications in Sustainable Energy and Environmental Remediation* (ACS Publications), 1–38. doi:10.1021/bk-2016-1238.ch001
- Sharma, R. K., Yadav, M., Monga, Y., Gaur, R., Adholeya, A., Zboril, R., et al. (2016c). Silica-Based Magnetic Manganese Nanocatalyst - Applications in the Oxidation of Organic Halides and Alcohols. *ACS Sustain. Chem. Eng.* 4 (3), 1123–1130. doi:10.1021/acssuschemeng.5b01183
- Siemen, P., Livingston, R. C., and Diederich, F. (2000). Acetylenic Coupling: a Powerful Tool in Molecular Construction. *Angew. Chem. Int. Ed.* 39 (15), 2632–2657. doi:10.1002/1521-3773(20000804)39:15<2632:aid-anie2632>3.0.co;2-f
- Sonogashira, K. (2002). Development of Pd–Cu Catalyzed Cross-Coupling of Terminal Acetylenes with Sp²-Carbon Halides. *J. Organomet. Chem.* 653 (1–2), 46–49. doi:10.1016/s0022-328x(02)01158-0
- Stang, P. J. (2008). *Metal-catalyzed Cross-Coupling Reactions*. John Wiley & Sons.
- Stang, P. J., and Tykwinski, R. R. (2006). *Acetylene Chemistry: Chemistry, Biology and Material Science*. John Wiley & Sons.
- Tartaglia, S., De Lucchi, O., and Gooßen, L. J. (2012). Practical Synthesis of Unsymmetrical Diarylacetylenes from Propiolic Acid and Two Different Aryl Bromides. *Eur. J. Org. Chem.* 2012 (7), 1431–1438. doi:10.1002/ejoc.201101770
- Tykwinski, R. R. (2003). Evolution in the Palladium-Catalyzed Cross-Coupling of Sp- and Sp²-Hybridized Carbon Atoms. *Angew. Chem. Int. Ed.* 42 (14), 1566–1568. doi:10.1002/anie.200201617
- Wang, D., and Astruc, D. (2014). Fast-Growing Field of Magnetically Recyclable Nanocatalysts. *Chem. Rev.* 114 (14), 6949–6985. doi:10.1021/cr500134h
- Wang, J., Zheng, S., Shao, Y., Liu, J., Xu, Z., and Zhu, D. (2010). Amino-functionalized Fe₃O₄@SiO₂ Core-Shell Magnetic Nanomaterial as a Novel Adsorbent for Aqueous Heavy Metals Removal. *J. Colloid Interf. Sci.* 349 (1), 293–299. doi:10.1016/j.jcis.2010.05.010
- Wang, S., Zhang, Z., Liu, B., and Li, J. (2013). Silica Coated Magnetic Fe₃O₄ Nanoparticles Supported Phosphotungstic Acid: a Novel Environmentally Friendly Catalyst for the Synthesis of 5-ethoxymethylfurfural from 5-hydroxymethylfurfural and Fructose. *Catal. Sci. Technol.* 3 (8), 2104–2112. doi:10.1039/c3cy00223c
- Wang, Z., Wang, X., Sun, H., Zhu, Z., Zhang, G., Zhang, W., et al. (2016). Triazine-Triazole Conjugates as Potent Ligands for Cu-Catalyzed Sonogashira Reaction. *ChemistrySelect* 1 (3), 391–395. doi:10.1002/slct.201600113
- Yamaura, M., Camilo, R., Sampaio, L., Macedo, M., Nakamura, M., and Toma, H. (2004). Preparation and Characterization of (3-aminopropyl) Triethoxysilane-Coated Magnetite Nanoparticles. *J. Magn. Magn. Mater.* 279 (2), 210–217. doi:10.1016/j.jmmm.2004.01.094
- Zhang, Q., Su, H., Luo, J., and Wei, Y. (2012). A Magnetic Nanoparticle Supported Dual Acidic Ionic Liquid: a “Quasi-Homogeneous” Catalyst for the One-Pot Synthesis of Benzoxanthenes. *Green. Chem.* 14 (1), 201–208. doi:10.1039/c1gc16031a
- Zhang, W.-W., Zhang, X.-G., and Li, J.-H. (2010). Palladium-catalyzed Decarboxylative Coupling of Alkynyl Carboxylic Acids with Benzyl Halides or Aryl Halides. *J. Org. Chem.* 75 (15), 5259–5264. doi:10.1021/jo1010284
- Zhang, Z., Zhang, F., Zhu, Q., Zhao, W., Ma, B., and Ding, Y. (2011). Magnetically Separable Polyoxometalate Catalyst for the Oxidation of Dibenzothiophene with H₂O₂. *J. Colloid Interf. Sci.* 360 (1), 189–194. doi:10.1016/j.jcis.2011.04.045
- Zhao, D., Gao, C., Su, X., He, Y., You, J., and Xue, Y. (2010). Copper-catalyzed Decarboxylative Cross-Coupling of Alkynyl Carboxylic Acids with Aryl Halides. *Chem. Commun.* 46 (47), 9049–9051. doi:10.1039/c0cc03772a
- Zhu, J., He, J., Du, X., Lu, R., Huang, L., and Ge, X. (2011). A Facile and Flexible Process of β-cyclodextrin Grafted on Fe₃O₄ Magnetic Nanoparticles and Host-Guest Inclusion Studies. *Appl. Surf. Sci.* 257 (21), 9056–9062. doi:10.1016/j.apsusc.2011.05.099

Conflict of Interest: The authors declare that the research was conducted in the absence of any commercial or financial relationships that could be construed as a potential conflict of interest.

Publisher’s Note: All claims expressed in this article are solely those of the authors and do not necessarily represent those of their affiliated organizations, or those of the publisher, the editors and the reviewers. Any product that may be evaluated in this article, or claim that may be made by its manufacturer, is not guaranteed or endorsed by the publisher.

Copyright © 2022 Yadav, Srivastava, Gaur, Gupta, Arora and Sharma. This is an open-access article distributed under the terms of the Creative Commons Attribution License (CC BY). The use, distribution or reproduction in other forums is permitted, provided the original author(s) and the copyright owner(s) are credited and that the original publication in this journal is cited, in accordance with accepted academic practice. No use, distribution or reproduction is permitted which does not comply with these terms.